INSTITUTE OF PHYSICS PUBLISHING JOURNAL OF PHYSICS A: MATHEMATICAL AND GENERAL

J. Phys. A: Math. Gen. **37** (2004) 6477–6489 PII: S0305-4470(04)76808-0

Universal mechanism for the intermittent route to strange nonchaotic attractors in quasiperiodically forced systems

Sang-Yoon Kim and Woochang Lim

Department of Physics, Kangwon National University, Chunchon, Kangwon-Do 200-701, Korea

E-mail: sykim@kangwon.ac.kr

Received 26 February 2004, in final form 4 May 2004
Published 9 June 2004
Online at stacks.iop.org/JPhysA/37/6477
doi:10.1088/0305-4470/37/25/004

Abstract

To examine the universality for the intermittent route to strange nonchaotic attractors (SNAs), we investigate the quasiperiodically forced Hénon map, ring map and Toda oscillator which are high-dimensional invertible systems. In these invertible systems, dynamical transition to an intermittent SNA occurs via a phase-dependent saddle–node bifurcation, when a smooth torus collides with a 'ring-shaped' unstable set. We note that this bifurcation mechanism for the appearance of intermittent SNAs is the same as that found in a simple system of the quasiperiodically forced noninvertible logistic map. Hence, the intermittent route to SNAs seems to be 'universal', in the sense that it occurs through the same mechanism in typical quasiperiodically forced systems of different nature.

PACS numbers: 05.45.Ac, 05.45.Df, 05.45.Pq

1. Introduction

Strange nonchaotic attractors (SNAs) typically appear in quasiperiodically forced dynamical systems [1]. These attractors were first described by Grebogi *et al* [2] and have been extensively investigated both theoretically [3–19] and experimentally [20]. SNAs exhibit some properties of regular as well as chaotic attractors. Like regular attractors, their dynamics is nonchaotic in the sense that they do not have a positive Lyapunov exponent; like usual chaotic attractors, they have a geometrically strange (fractal) structure. Moreover, SNAs are related to the Anderson localization in the Schrödinger equation with a quasiperiodic potential [21], and they may have a practical application in secure communication [22]. Hence, dynamical routes to SNAs have become a topic of considerable current interest.

Here, we are interested in the dynamical route to SNAs accompanied by intermittent behaviour [13]. As a parameter passes a threshold value, a smooth torus abruptly transforms into an intermittent SNA. This route to an intermittent SNA is quite general and has been observed in a number of quasiperiodically forced period-doubling systems (e.g., see [14, 15]). Recently in [19], the bifurcation mechanism for the intermittent route to SNAs has been investigated in a simple model of the quasiperiodically forced noninvertible logistic map. Here, to examine the universality for the intermittent transition to SNAs, we investigate the mechanism for the appearance of intermittent SNAs in quasiperiodically forced invertible systems of different nature.

This paper is organized as follows. In section 2, we study the mechanism for the intermittent route to SNAs in the quasiperiodically forced Hénon map, ring map and Toda oscillator which are high-dimensional invertible period-doubling systems. In all systems we study, a transition from a smooth torus to an intermittent SNA is found to take place through a 'phase-dependent' saddle–node bifurcation between a smooth torus (corresponding to a two-frequency quasiperiodic attractor) and a new type of invariant 'ring-shaped' unstable set. Note that this bifurcation mechanism for the intermittent route to SNAs is the same as that found in the quasiperiodically forced noninvertible logistic map [19]. Hence, the intermittent transition to SNAs seems to be a universal one because it occurs through the same mechanism in a large class of quasiperiodically forced period-doubling systems. Finally, a summary is given in section 3.

2. Mechanism for the intermittent transition to strange nonchaotic attractors

In this section, we investigate invertible systems of different nature such as the quasiperiodically forced Hénon map, ring map and Toda oscillator and examine the universality for the intermittent route to SNAs.

2.1. Intermittent SNAs in the quasiperiodically forced Hénon map

As a first example, we consider the quasiperiodically forced Hénon map [7], often used as a representative model for the Poincaré maps of quasiperiodically forced oscillators:

$$M: \quad \begin{cases} x_{n+1} = a - x_n^2 + y_n + \varepsilon \cos 2\pi\theta_n \\ y_{n+1} = bx_n \\ \theta_{n+1} = \theta_n + \omega \ (\mathrm{mod}\ 1) \end{cases} \tag{1}$$

where a is the nonlinearity parameter of the unforced Hénon map and ω and ε represent the frequency and amplitude of the quasiperiodic forcing, respectively. This quasiperiodically forced Hénon map M is invertible, because it has a nonzero constant Jacobian determinant $-b$ whose magnitude is less than unity (i.e., $b \neq 0$ and $-1 < b < 1$). Here, we fix the value of the dissipation parameter b at $b = 0.05$ and set the frequency ω to be the reciprocal of the golden mean, $\omega = (\sqrt{5} - 1)/2$. Then, using the rational approximations (RAs) to this quasiperiodic forcing, we investigate the intermittent route to SNAs. For the inverse golden mean, its rational approximants are given by the ratios of the Fibonacci numbers, $\omega_k = F_{k-1}/F_k$, where the sequence of $\{F_k\}$ satisfies $F_{k+1} = F_k + F_{k-1}$ with $F_0 = 0$ and $F_1 = 1$. Instead of the quasiperiodically forced system, we study an infinite sequence of periodically forced systems with rational driving frequencies ω_k. We suppose that the properties of the original system M may be obtained by taking the quasiperiodic limit $k \to \infty$.

Figure 1(a) shows a phase diagram in the a–ε plane. Each phase is characterized by both the (nontrivial) Lyapunov exponents, σ_1 and σ_2 ($\leqslant \sigma_1$), associated with dynamics of the

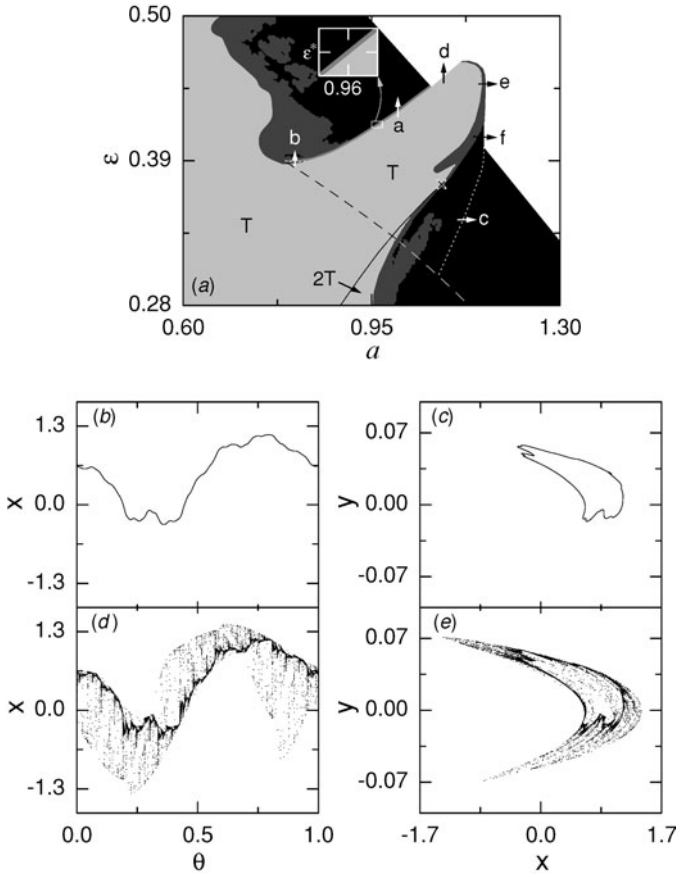

Figure 1. (*a*) Phase diagram of the quasiperiodically forced Hénon map in the a–ε plane for the case of $b = 0.05$ and $\omega = (\sqrt{5} - 1)/2$. Regular, chaotic, SNA and divergence regimes are shown in light gray, black, gray (or dark gray) and white, respectively. To show the region of existence (gray) of the intermittent SNA occurring between T (light gray) and the chaotic attractor region (black), a small box near $(a, \varepsilon) = (0.96, \varepsilon^*$ (=0.416 857 986)) is magnified. Through interaction with the ring-shaped unstable set born when passing the dashed line (which is obtained for a sufficiently large level $k = 10$ of the RAs), typical dynamical transitions such as the intermittency (route a) and the interior (routes b and c; the dotted line is an interior crisis line) and boundary (routes d, e and f) crises may occur. Here, the torus and the doubled torus are denoted by T and $2T$ and the solid line represents a torus-doubling bifurcation curve whose terminal point is marked with the cross. Projections of a smooth torus onto (*b*) the θ–x and (*c*) x–y planes for $a = 0.96$. In (*b*) and (*c*), the initial orbit points are $(x_0, y_0, \theta_0) = (0.8, 0.0, 0.0)$, 5×10^3 points are computed before plotting, and the next 10^4 points are plotted. Projections of an SNA onto (*d*) the θ–x and (*e*) x–y planes for $a = 0.96\,\varepsilon = 0.416\,86$. In (*d*) and (*e*), the initial orbit points are $(x_0, y_0, \theta_0) = (0.8, 0.0, 0.0)$, 5×10^3 points are computed before plotting, and the next 6×10^4 points are plotted. For other details, see the text.

variables x and y (besides the zero exponent, related to the phase variable θ of the quasiperiodic forcing) and the phase sensitivity exponent δ. The exponent δ measures the sensitivity with respect to the phase of the quasiperiodic forcing and characterizes the strangeness of an attractor [6]. A smooth torus has negative Lyapunov exponents ($\sigma_{1,2} < 0$) and has no phase sensitivity (i.e., $\delta = 0$). The region where it exists is shown in light gray and represented by T. When crossing the solid line, the smooth torus becomes unstable and a smooth doubled

torus appears in the region denoted by $2T$. On the other hand, a chaotic attractor has a positive Lyapunov exponent $\sigma_1 > 0$, and its region is shown in black. Between these regular and chaotic regions, SNAs that have negative Lyapunov exponents ($\sigma_{1,2} < 0$) and positive phase sensitivity exponents ($\delta > 0$) exist in the regions shown in gray and dark gray. Due to their high phase sensitivity, SNAs have a strange fractal structure. In the thin gray region (e.g., see a magnified part in figure 1(a)), intermittent SNAs exist, while in the dark gray region nonintermittent SNAs, born through the mechanism of the gradual fractalization [11] or torus collision [5], exist.

A main interesting feature of the phase diagram is the existence of the 'tongue' of quasiperiodic motion that penetrates into the chaotic region and separates it into upper and lower parts. This tongue lies near the terminal point (represented by the cross) of the torus doubling bifurcation curve. Upon crossing the upper boundary of the tongue, a smooth torus transforms into an intermittent SNA that exists in the thin gray region. Here, we investigate this intermittent route to SNAs (see the route a in figure 1(a)). As an example, consider the case of $a = 0.96$. Figures 1(b) and (c) show projections of a smooth torus with $\sigma_1 = -0.077$ onto the θ–x and x–y planes for $\varepsilon = 0.415$, respectively. We note that the projections are smooth invariant curves. A curve can be regarded as a cross section (Poincaré map) for the two-frequency quasiperiodic motion on a smooth torus in continuous-time dynamical systems. Hence, we call this curve a torus. However, as ε passes a threshold value ε^* (=0.416 857 986), dynamical transition to an intermittent SNA, occupying a finite volume of the phase space, occurs. As shown in figures 1(d) and (e) for $\varepsilon = 0.416\,86$, a typical trajectory on the newly born intermittent SNA with $\sigma_1 = -0.006$ and $\delta = 4.32$ spends most of its time near the former torus with sporadic large bursts away from it.

Using RAs, we search for an unstable orbit that causes the intermittent transition via a collision with the smooth (stable) torus. Thus, an invariant 'ring-shaped' unstable set that is different from the smooth unstable torus is found. When crossing the dashed curve in figure 1, such a ring-shaped unstable set appears through a phase-dependent saddle–node bifurcation which has no counterpart in the unforced case. As an example, consider the RA of level $k = 7$. The RA to the smooth torus (denoted by a black line), composed of stable orbits with period F_7 (=13), is shown in figure 2(a) for $a = 0.85$ and $\varepsilon = 0.3707$. We note that a ring-shaped unstable set, born via a phase-dependent saddle–node bifurcation and composed of F_7 small rings, lies near the smooth torus. At first, each ring is composed of the stable (shown in black) and unstable (shown in gray) orbits with period F_7 (see the inset in figure 2(a)). However, as the parameters increase such rings make evolution, as shown in figure 2(b), for $a = 0.86$ and $\varepsilon = 0.375$. For fixed values of a and ε, the phase θ may be regarded as a 'bifurcation parameter'. As θ is changed, a chaotic attractor appears via an infinite sequence of period-doubling bifurcations of stable periodic orbits in each ring, and then it disappears via a boundary crisis when it collides with the unstable F_7-periodic orbit (see the inset in figure 2(b)). Thus, the attracting part (shown in black) of each ring is composed of the union of the originally stable F_7-periodic attractor and the higher $2^n F_7$-periodic ($n = 1, 2, \ldots$) and chaotic attractors born through the period-doubling cascade. On the other hand, the unstable part (shown in gray) of each ring consists of the union of the originally unstable F_7-periodic orbit (e.g., the upper gray line in the inset in figure 2(b)) born via a saddle–node bifurcation and the destabilized F_7-periodic orbit (e.g., the lower gray line in the inset in figure 2(b)) via a period-doubling bifurcation. As the parameters are further increased, both the size and shape of the rings change, and for sufficiently large parameters, each ring is composed of a large unstable part (shown in gray) and a small attracting part (shown in black), as shown in figure 2(c) for $a = 0.96$ and $\varepsilon = 0.4$. Furthermore, new rings may appear inside or outside the 'old' rings via another (phase-dependent) saddle–node bifurcation (e.g., see F_7 new small

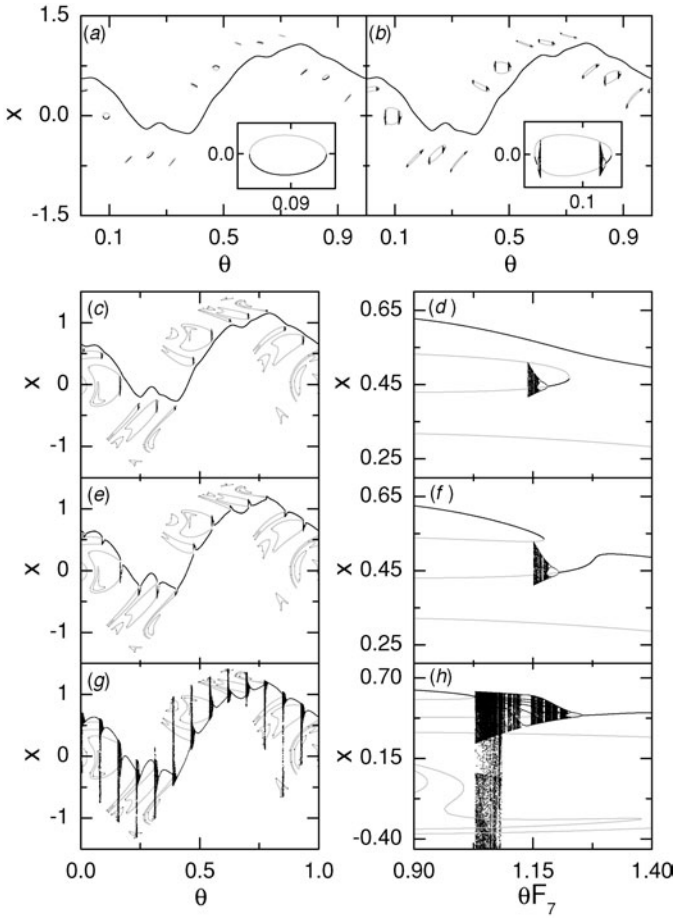

Figure 2. Dynamical mechanism for the intermittent route to SNAs in the quasiperiodically forced Hénon map. In (*a*)–(*h*), projections of the attractor and the ring-shaped unstable set onto the θ–x plane are given in the RA of level 7. A smooth torus (denoted by a black curve) and a ring-shaped unstable set (composed of F_7 (=13) rings) are shown for (*a*) $a = 0.85$ and $\varepsilon = 0.3707$ and (*b*) $a = 0.86$ and $\varepsilon = 0.375$. Each ring is composed of the attracting part (shown in black) and the unstable part (shown in gray and consisting of unstable F_7-periodic orbits). Magnified views of rings are given in insets. In (*c*), a ring-shaped unstable set (composed of $2F_7$ (=26) rings) lies close to the smooth torus (denoted by a black curve) for $a = 0.96$ and $\varepsilon = 0.4$. A magnified view near $(\theta F_7, x) = (1.15, 0.45)$ is given in (*d*). For this case, the intermittent transition from a smooth torus to an SNA occurs through the following two procedures. First, the RA to the attractor becomes nonsmooth via a phase-dependent saddle–node bifurcation, as shown in (*e*) (a magnified view is given in (*f*)) for $a = 0.96$ and $\varepsilon = 0.4015$. Second, the chaotic component in the RA to the attractor becomes suddenly widened via an interior crisis, as shown in (*g*) (a magnified view is given in (*h*)) for $a = 0.96$ and $\varepsilon = 0.4045$. Thus, F_7 'gaps', filled by intermittent chaotic attractors, are formed. For more details, see the text.

rings in figure 2(*c*)). With further increase in the level k of the RAs, the ring-shaped unstable set consists of a larger number of rings with a smaller attracting part. Hence, we believe that, in the quasiperiodic limit, the ring-shaped unstable set might become a complicated invariant unstable set composed of only unstable orbits.

In terms of the RA of level 7, we now explain the mechanism for the intermittent transition occurring in figures 1(*b*)–(*e*) for $a = 0.96$. As we approach the border of the intermittent

transition in the phase diagram, the ring-shaped unstable set comes closer to the smooth torus (denoted by a black curve), as shown in figure 2(*c*) for $\varepsilon = 0.4$ (a magnified view is given in figure 2(*d*)). As ε passes a threshold value $\varepsilon_7^{(1)}$ (=0.401 035 615), a phase-dependent saddle–node bifurcation occurs between the smooth torus and the unstable part (shown in gray) of the ring-shaped unstable set. Then, the new attractor of the system contains the attracting part (shown in black) of the ring-shaped unstable set and becomes nonsmooth, which is shown in figure 2(*e*) for $\varepsilon = 0.4015$ (see a magnified view in figure 2(*f*)). As ε is further increased, the chaotic component in the RA to the attractor increases, and eventually for $\varepsilon_7^{(2)} = 0.403\,399\,486$, it becomes suddenly widened via an interior crisis when it collides with the nearest ring (e.g., see figure 2(*g*) for $\varepsilon = 0.4045$). Then, F_7 (=13) 'gaps', where no attractors with period F_7 exist, are formed. A magnified gap is shown in figure 2(*h*). Note that this gap is filled by intermittent chaotic attractors. This RA to the whole attractor consists of the union of the periodic and chaotic components. For this case, the periodic component dominates, and hence the average first Lyapunov exponent ($\langle\sigma_1\rangle = -0.168$) becomes negative, where $\langle\cdots\rangle$ denotes the average over the whole θ. Hence, the RA to the attractor becomes nonchaotic. We note that this seventh RA to the attractor in figure 2(*g*) resembles the (original) intermittent SNA in figure 1(*d*), although the level of the RA is low. Thus, in the RAs the intermittent transition to an SNA consists of two stages: the phase-dependent saddle–node bifurcation and the interior crisis. This is in contrast to the previously reported case in the quasiperiodically forced logistic map [19], where the intermittent transition occurs directly through only the phase-dependent saddle–node bifurcation. Increasing the level to $k = 18$, we obtain the threshold values $\varepsilon_k^{(1)}$ and $\varepsilon_k^{(2)}$ at which the phase-dependent saddle–node bifurcation and the interior crisis occur, respectively. As the level k increases, the difference $\Delta\varepsilon_k \left(\equiv \varepsilon_k^{(2)} - \varepsilon_k^{(1)}\right)$ tends to zero, and both sequences of $\left\{\varepsilon_k^{(1)}\right\}$ and $\left\{\varepsilon_k^{(2)}\right\}$ converge to the same quasiperiodic limit ε^* (=0.416 857 986) in an algebraic manner, $\left|\Delta\varepsilon_k^{(i)}\right| \left(\equiv \left|\varepsilon_k^{(i)} - \varepsilon^*\right|\right) \sim F_k^{-\alpha}$ ($i = 1, 2$), where $\alpha \simeq 2.0$, as shown in figure 3. In the quasiperiodic limit $k \to \infty$, the RA to the attractor has a dense set of gaps which are filled by intermittent chaotic attractors. Consequently, an intermittent SNA, containing the whole ring-shaped unstable set, appears, as shown in figure 1(*d*). As ε is further increased and passes another threshold value ε^c (=0.416 879), the SNA transforms into a chaotic attractor.

2.2. Intermittent SNAs in the quasiperiodically forced ring map

As a second example, we consider the quasiperiodically forced ring map [7],

$$M: \quad \begin{cases} x_{n+1} = x_n + \Omega - \dfrac{a}{2\pi}\sin 2\pi x_n + by_n + \varepsilon\cos 2\pi\theta_n \pmod 1 \\ y_{n+1} = by_n - \dfrac{a}{2\pi}\sin 2\pi x_n \\ \theta_{n+1} = \theta_n + \omega \pmod 1 \end{cases} \tag{2}$$

where a quasiperiodic forcing of the frequency ω and amplitude ε is acted on the two-dimensional ring map with the parameters of the nonlinearity a and phase shift Ω. This quasiperiodically forced ring map is an invertible dissipative map because it has a nonzero constant Jacobian determinant b ($b \neq 0$ and $-1 < b < 1$). (In the singular limit of $b = 0$, this map is reduced to the quasiperiodically forced circle map [8].) Here, the value of b is fixed at $b = 0.01$. This system M may be used as a model for the quasiperiodically forced pendulum, Josepson junction and charge-density wave [23].

We consider the case of $\Omega = 0$. For this case, the quasiperiodically forced ring map has a symmetry because it is invariant under the transformation,

$$S: x \to -x \qquad y \to -y \qquad \text{and} \qquad \theta \to \theta + 1/2. \tag{3}$$

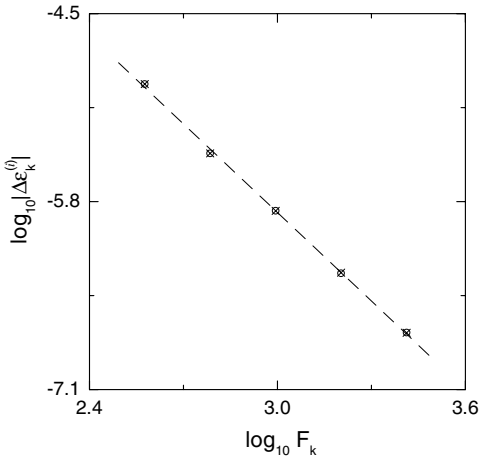

Figure 3. Plot of $\log_{10}|\Delta\varepsilon_k^{(i)}|$ versus $\log_{10} F_k$ for $k = 14, \ldots, 18$ ($\Delta\varepsilon_k^{(i)} = \varepsilon_k^{(i)} - \varepsilon^*, i = 1$ (circles) and $i = 2$ (crosses)). Here, $\varepsilon_k^{(1)}$ and $\varepsilon_k^{(2)}$ represent the threshold values for the saddle–node bifurcation and the interior crisis in the RA of level k, respectively, and ε^* denotes the quasiperiodic limit.

Here, we set ω to be the reciprocal of the golden mean (i.e., $\omega = (\sqrt{5}-1)/2$), and investigate the transition to intermittent SNAs by using the RAs. Figure 4(a) shows a phase diagram in the a–ε plane, where all phases are symmetric ones. Each dynamical phase is characterized by calculating both the nontrivial Lyapunov exponents, σ_1 and σ_2, associated with dynamics of the variables x and y and the phase sensitivity exponent δ. As in the quasiperiodically forced Hénon map, a tongue of quasiperiodic motion, penetrating into the chaotic region, lies near the terminal point (denoted by the cross) of the torus doubling bifurcation line (represented by the solid line). When crossing the upper boundary of the tongue (see the route a in figure 4(a)), a transition to an intermittent SNA occurs. As an example, we consider the case of $a = 2.95$. For $\varepsilon = 0.1801$, a symmetric smooth torus with $\sigma_1 = -0.069$ exists, as shown in figure 4(b). However, as ε passes a threshold value ε^* (=0.180 275 991), dynamical transition to a symmetric intermittent SNA occurs (e.g., see the SNA with $\sigma_1 = -0.004$ and $\delta \simeq 20.5$ in figure 4(c) for $\varepsilon = 0.180\,276$).

We now use the RA of level 7 and explain the mechanism for the intermittent route to SNAs occurring for $a = 2.95$. Since the driving period F_7 (=13) is an odd number, all orbits, constituting the RAs to the symmetric attractor and the symmetric ring-shaped unstable set, are asymmetric ones with respect to the θ-transformation in S of equation (3). However, such RAs are symmetric because they contain all conjugate pairs of asymmetric orbits in the whole range of θ ($0 \leqslant \theta < 1$). This is in contrast to the case of even driving periods, where all orbits in the RAs are symmetric ones. Figure 5(a) shows that a ring-shaped unstable set, composed of $14F_7$ (=182) rings, lies close to the smooth torus (denoted by a black curve) for $\varepsilon = 0.177$. In a basic interval of $\theta F_7 \in [0.2, 1.2)$, a magnified view of conjugate pairs of asymmetric orbits (the nearest orbit point conjugate to an asymmetric orbit point lying at a given θF_7 lies at $\theta F_7 + 1/2$), constituting the smooth torus and the ring-shaped unstable set, is shown in figure 5(b). As ε passes a threshold value $\varepsilon_7^{(1)}$ (=0.177 196 924), a pair of phase-dependent saddle–node bifurcations occurs through the collision of the smooth torus and the unstable part (shown in gray) of the ring-shaped unstable set. Consequently, the RA to the new attractor, containing the attracting part (shown in black) of the ring-shaped unstable

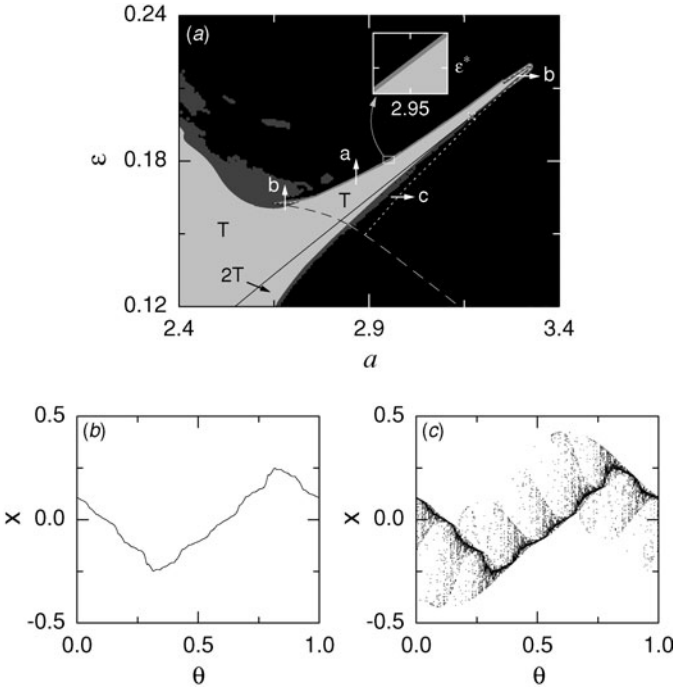

Figure 4. (a) Phase diagram of the quasiperiodically forced ring map in the a–ε plane for the case of $b = 0.01$ and $\omega = (\sqrt{5} - 1)/2$. In the thin gray region, intermittent SNAs exist, while in the dark gray region, nonintermittent SNAs exist. Here, all phases are symmetric. Regular, chaotic and SNA regimes are shown in light gray, black and gray (or dark gray), respectively. To show the region of existence (gray) of the intermittent SNA occurring between T (light gray) and the chaotic attractor region (black), a small box near $(a, \varepsilon) = (2.95, \varepsilon^*\ (=0.180\,275\,991))$ is magnified. Through interaction with the ring-shaped unstable set born when passing the dashed line, typical dynamical transitions such as the intermittency (route a) and the interior crisis (routes b and c; the dotted line is an interior crisis line) may occur. Here, the torus and the doubled torus are denoted by T and $2T$ and the solid line represents a torus doubling bifurcation curve whose terminal point is marked with the cross. Projections of (b) the symmetric smooth torus for $a = 2.95$ and $\varepsilon = 0.1801$ and (c) the symmetric intermittent SNA for $a = 2.95$ and $\varepsilon = 0.180\,276$ onto the θ–x plane are shown. In (b) or (c), the initial orbit point is $(x_0, y_0, \theta_0) = (0.0, 0.0, 0.0)$, 5×10^3 points are computed before plotting, and the next 10^4 (6×10^4) points are plotted. For other details, see the text.

set, becomes nonsmooth, as shown in figures 5(c) and (d) for $\varepsilon = 0.1775$. As ε passes another threshold value $\varepsilon_7^{(2)}$ (=0.177 855 989), the chaotic component in the RA becomes abruptly widened via a pair of interior crises (e.g., see figure 5(e) for $\varepsilon = 0.178$). Then, 'gaps' without F_7-periodic attractors are formed and they are filled by intermittent chaotic attractors. Figure 5(f) shows a conjugate pair of asymmetric gaps in a basic interval of $\theta F_7 \in [0.2, 1.2)$. Hence, the RA to the whole attractor contains $2F_7$ (=26) gaps. This is in contrast to the case of the quasiperiodically forced Hénon map without symmetry, where only F_7 gaps appear through the interior crisis (see figure 2(g)). Furthermore, the RA to the whole attractor becomes nonchaotic because its average first Lyapunov exponent is $\langle\sigma_1\rangle = -0.053$. We note that this seventh RA to the attractor in figure 5(e) is similar to the (original) intermittent SNA in figure 4(c) although the level of the RA is low. By increasing the level to $k = 16$, we get the threshold values $\varepsilon_k^{(1)}$ and $\varepsilon_k^{(2)}$ at which the phase-dependent saddle–node bifurcation and the interior crisis occur, respectively. It is thus found that as the level k increases, both

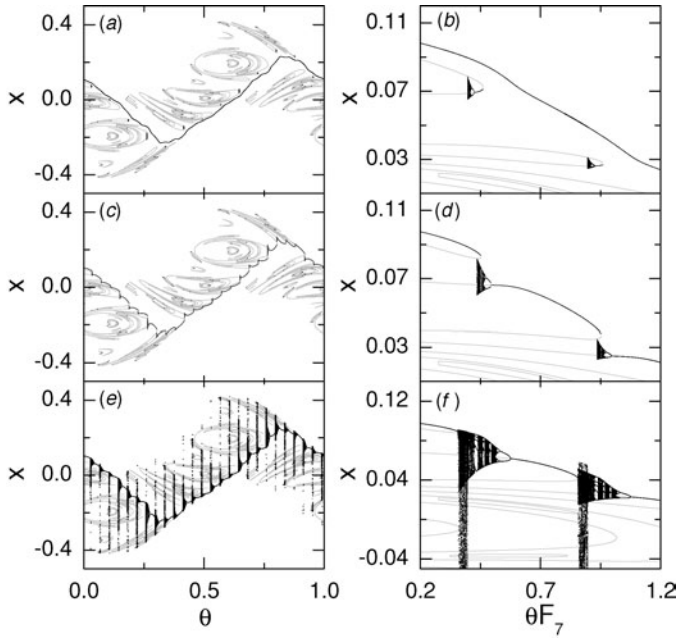

Figure 5. Intermittent route to SNAs for $a = 2.95$ in the quasiperiodically forced ring map. In (a)–(f), projections of the attractor and the ring-shaped unstable set onto the θ–x plane are given in the RA of level 7. In (a), a symmetric ring-shaped unstable set (composed of $14F_7$ (=182) rings) lies close to a symmetric smooth torus (denoted by a black curve) for $\varepsilon = 0.177$. A magnified view near $(\theta F_7, x) = (0.7, 0.07)$ is given in (b). In the RA, the intermittent transition from the symmetric smooth torus to a symmetric SNA occurs through the following two stages. First, the RA to the attractor becomes nonsmooth via a pair of phase-dependent saddle–node bifurcations, as shown in (c) (a magnified view is given in (d)) for $\varepsilon = 0.1775$. Second, the chaotic component in the RA to the attractor becomes suddenly widened via a pair of interior crises, as shown in (e) (a magnified view is given in (f)) for $\varepsilon = 0.178$. Thus, $2F_7$ (=26) 'gaps', filled by intermittent chaotic attractors, are formed. For more details, see the text.

sequences of $\{\varepsilon_k^{(1)}\}$ and $\{\varepsilon_k^{(2)}\}$ converge to the same quasiperiodic limit ε^* (=0.180 275 991) in an algebraic way, $|\Delta\varepsilon_k^{(i)}| \left(\equiv|\varepsilon_k^{(i)} - \varepsilon^*|\right) \sim F_k^{-\alpha}$ ($i = 1, 2$), where $\alpha \simeq 2.0$. Note that the value of α is the same as that in the quasiperiodically forced Hénon map. In the quasiperiodic limit $k \to \infty$, the RA to the attractor has a dense set of gaps filled by intermittent chaotic attractors. Consequently, a symmetric intermittent SNA, containing the whole ring-shaped unstable set, appears when passing the threshold value ε^*, as shown in figure 4(c). This intermittent SNA transforms into a symmetric chaotic attractor as ε passes another threshold value ε^c (=0.185 276 21).

2.3. Intermittent SNAs in the quasiperiodically forced Toda oscillator

As a third example, we consider the Toda oscillator with an asymmetric exponential potential [24] which is quasiperiodically forced at two incommensurate frequencies,

$$\ddot{x} + \gamma\dot{x} + e^x - 1 = a\cos\omega_1 t + \varepsilon\cos\omega_2 t \tag{4}$$

where γ is the damping coefficient, a and ε represent the amplitudes of the quasiperiodic forcing and $\omega\,(\equiv\omega_2/\omega_1)$ is irrational. By making a normalization, $\omega_1 t \to 2\pi t$, equation (4)

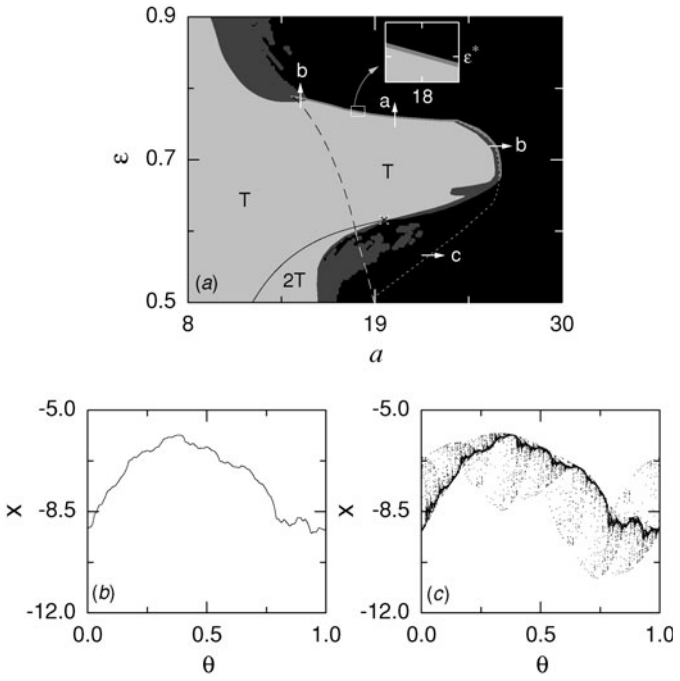

Figure 6. (*a*) Phase diagram of the quasiperiodically forced Toda oscillator in the a–ε plane for the case of $\gamma = 0.8$, $\omega_1 = 2.0$ and $\omega = (\sqrt{5}-1)/2$. Regular, chaotic and SNA regimes are shown in light gray, black and gray (or dark gray), respectively. In the thin gray region, intermittent SNAs exist, while in the dark gray region, nonintermittent SNAs exist. To show the region of existence (gray) of the intermittent SNA occurring between T (light gray) and the chaotic attractor region (black), a small box near $(a, \varepsilon) = (18, \varepsilon^*\ (=0.765\,139\,585))$ is magnified. Through interaction with the ring-shaped unstable set born when passing the dashed line, typical dynamical transitions such as the intermittency (route a) and the interior crisis (routes b and c; the dotted line is an interior crisis line) may occur. Here, the torus and the doubled torus are denoted by T and $2T$ and the solid line represents a torus doubling bifurcation curve whose terminal point is marked with the cross. Projections of (*b*) the smooth torus for $a = 18$ and $\varepsilon = 0.764$ and (*c*) the intermittent SNA for $a = 18$ and $\varepsilon = 0.765\,15$ onto the θ–x plane are shown. In (*b*) or (*c*), the initial orbit point is $(x_0, y_0, \theta_0) = (-8, 8, 0)$, 5×10^3 points are computed before plotting, and the next 10^4 (6×10^4) points are plotted. For other details, see the text.

can be reduced to three first-order differential equations,

$$\dot{x} = y \qquad \dot{y} = -\frac{2\pi}{\omega_1}\gamma y + \frac{4\pi^2}{\omega_1^2}(-\mathrm{e}^x + 1 + a\cos 2\pi t + \varepsilon \cos 2\pi\theta) \qquad \dot{\theta} = \omega \ (\mathrm{mod}\ 1). \tag{5}$$

This system may be used as a model for the quasiperiodically forced RLC circuit [25].

The phase space of the quasiperiodically forced Toda oscillator is four-dimensional with coordinates x, y, θ and t. Since the system is periodic in t, it is convenient to regard time as a circular coordinate in the phase space. Then, we consider the surface of section, the x–y–θ hypersurface at integer times (i.e., $t = n$, where n is the integer). The phase-space trajectory intersects the surface of section in a sequence of points. This sequence of points corresponds to a mapping on the 3D hypersurface. The map can be computed by stroboscopically sampling the orbit points $\mathbf{v}_n\ (\equiv (x_n, y_n, \theta_n))$ at the discrete time n. We call the transformation $\mathbf{v}_n \to \mathbf{v}_{n+1}$ the Poincaré map, and write $\mathbf{v}_{n+1} = P(\mathbf{v}_n)$. This 3D Poincaré map P has a constant Jacobian determinant of $\mathrm{e}^{-\gamma T_1}$, where $T_1 = 2\pi/\omega_1$.

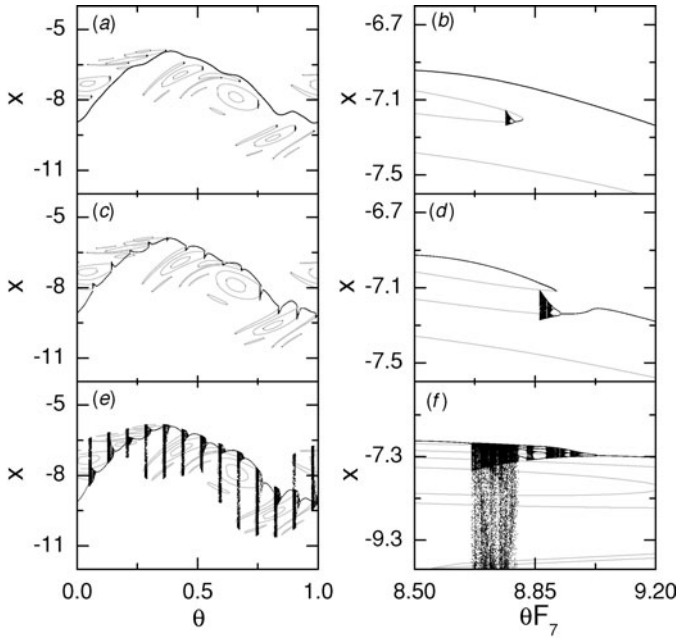

Figure 7. Intermittent route to SNAs for $a = 18$ in the quasiperiodically forced Toda oscillator. In (a)–(f), projections of the attractor and the ring-shaped unstable set onto the θ–x plane are given in the RA of level 7. In (a), the ring-shaped unstable set (composed of $2F_7$ (=26) rings) lies close to the smooth torus (denoted by a black curve) for $\varepsilon = 0.715$. A magnified view near $(\theta F_7, x) = (8.85, -7.1)$ is given in (b). In the RA, the intermittent transition from a smooth torus to an SNA occurs through the following two stages. First, the RA to the attractor becomes nonsmooth via a phase-dependent saddle–node bifurcation, as shown in (c) (a magnified view is given in (d)) for $\varepsilon = 0.729$. Second, the chaotic component in the RA to the attractor becomes abruptly widened via an interior crises, as shown in (e) (a magnified view is given in (f)) for $\varepsilon = 0.74$. Thus, F_7 (=13) 'gaps', filled by intermittent chaotic attractors, are formed. For more details, see the text.

Here, we set ω to be the reciprocal of the golden mean (i.e., $\omega = (\sqrt{5} - 1)/2)$), and investigate the intermittent route to SNAs in the 3D Poincaré map P for the case of $\gamma = 0.8$ and $\omega_1 = 2.0$. Figure 6(a) shows a phase diagram in the a–ε plane. Here, each dynamical phase is characterized in terms of the nontrivial Lyapunov exponents, σ_1 and σ_2 (associated with dynamics of the variables x and y), and the phase sensitivity exponent δ. As in the preceding examples, a tongue of quasiperiodic motion, penetrating into the chaotic region, exists near the terminal point (denoted by the cross) of the torus-doubling bifurcation curve (represented by the solid line). When crossing the upper boundary of the tongue (see the route a in figure 6(a)), an intermittent transition to an SNA takes place. As an example, we consider the case of $a = 18$. For $\varepsilon = 0.764$, a smooth torus with $\sigma_1 = -0.043$ exists, as shown in figure 6(b). However, when passing a threshold value ε^*(=0.765 139 585), dynamical transition to an intermittent SNA occurs (e.g., see the SNA with $\sigma_1 = -0.004$ and $\delta \simeq 7.6$ in figure 6(c) for $\varepsilon = 0.765\,15$).

Using the RA of level 7, we explain the mechanism for the intermittent transition to SNAs occurring for $a = 18$. As ε is increased towards a threshold value $\varepsilon_7^{(1)}$ (=0.727 986 519), the ring-shaped unstable set, composed of $2F_7$ (=26) rings, comes closer to the smooth torus (denoted by a black curve), as shown in figure 7(a) for $\varepsilon = 0.715$ (a magnified view is given in figure 7(b)). When passing the threshold value $\varepsilon_7^{(1)}$, a phase-dependent saddle–node bifurcation

occurs between the smooth torus and the unstable part (shown in gray) of the ring-shaped unstable set. Then, the smooth torus is broken, and a nonsmooth attractor, containing the attracting part (shown in black) of the ring-shaped unstable set, appears (e.g., see figures 7(c) and (d) for $\varepsilon = 0.729$). As ε is further increased, the chaotic component in the RA to the attractor increases, and eventually for $\varepsilon_7^{(2)} = 0.734\,049\,948$, it becomes abruptly widened via an interior crisis (e.g., see figure 7(e) for $\varepsilon = 0.74$). Then, F_7 'gaps' without F_7-periodic attractors appear. Figure 7(f) shows a magnified gap, filled by intermittent chaotic attractors. Moreover, the RA to the attractor is nonchaotic because $\langle\sigma_1\rangle = -0.102$. We note that the seventh RA to the attractor in figure 7(e) resembles the (original) intermittent SNA in figure 6(c) although the level of the RA is low. Increasing the level to $k = 15$, we obtain the threshold values $\varepsilon_k^{(1)}$ and $\varepsilon_k^{(2)}$ at which the phase-dependent saddle–node bifurcation and the interior crisis occur, respectively. As the level k increases, both sequences of $\{\varepsilon_k^{(1)}\}$ and $\{\varepsilon_k^{(2)}\}$ are found to converge to the same quasiperiodic limit ε^* (=0.765 139 585) in an algebraic way, $|\Delta\varepsilon_k^{(i)}|\ (\equiv|\varepsilon_k^{(i)} - \varepsilon^*|) \sim F_k^{-\alpha}$ ($i = 1, 2$), where $\alpha \simeq 2.0$. We note that the value of α is the same as that in the preceding examples within numerical accuracy[1]. In the quasiperiodic limit $k \to \infty$, the RA to the attractor has a dense set of gaps filled by intermittent chaotic attractors. As a result, an intermittent SNA, containing the whole ring-shaped unstable set, appears, as shown in figure 6(c). As ε is further increased, the value of $\langle\sigma_1\rangle$ of the SNA increases, and eventually for $\varepsilon = \varepsilon^c$ (=0.765 154), it becomes zero. Then, a transition to chaos occurs.

3. Summary

To examine the universality for the intermittent route to SNAs, we have studied the mechanism for the appearance of intermittent SNAs in quasiperiodically forced invertible period-doubling systems such as the quasiperiodically forced Hénon map, ring map and Toda oscillator. A common feature of the phase diagrams of these period-doubling systems is that a tongue of quasiperiodic motion, penetrating into the chaotic region, exists near the terminal point of the torus-doubling bifurcation line. We believe that this tongue structure might be typical for quasiperiodically forced period-doubling systems. Interestingly, when passing the upper boundary of the tongue, a smooth torus transforms into an intermittent SNA. Using the RAs to the quasiperiodic forcing, we have investigated the mechanism for this intermittent transition to SNAs. Thus, it has been found that, when a smooth torus makes a collision with a ring-shaped unstable set, dynamical transition to an intermittent SNA occurs via a phase-dependent saddle–node bifurcation in all invertible systems we have studied. We note that this bifurcation mechanism for the appearance of intermittent SNAs is the same as that in the quasiperiodically forced noninvertible logistic map. Hence, the intermittent route to SNAs seems to be universal, since it occurs through the same mechanism in typical quasiperiodically forced period-doubling systems of different nature.

Acknowledgments

SYK thanks Dr A Jalnine for fruitful discussions on dynamical transitions in quasiperiodically forced systems. This work was supported by the 2003 Research Program of the Kangwon National University.

[1] For clear understanding of the numerical result of the exponent α, a theoretical investigation for α is necessary. However, such a work is beyond the scope of the present work, and hence it will be done in future.

References

[1] Prasad A, Negi S S and Ramaswamy R 2001 *Int. J. Bif. Chaos* **11** 291
[2] Grebogi C, Ott E, Pelikan S and Yorke J A 1984 *Physica* D **13** 261
[3] Romeiras F J and Ott E 1987 *Phys. Rev.* A **35** 4404
Ding M, Grebogi C and Ott E 1989 *Phys. Rev.* A **39** 2593
[4] Kapitaniak T, Ponce E and Wojewoda T 1990 *J. Phys.* A **23** L383
[5] Heagy J F and Hammel S M 1994 *Physica* D **70** 140
[6] Pikovsky A S and Feudel U 1995 *Chaos* **5** 253 (see equations (11)–(14) for the definition of the phase sensitivity exponent δ)
[7] Sosnovtseva O, Feudel U, Kurths J and Pikovsky A 1996 *Phys. Lett.* A **218** 255
[8] Feudel U, Kurths J and Pikovsky A S 1995 *Physica* D **88** 176
Feudel U, Grebogi C and Ott E 1997 *Phys. Rep.* **290** 11
[9] Kuznetsov S P, Pikovsky A S and Feudel U 1995 *Phys. Rev.* E **51** R1629
Kuznetsov S, Feudel U and Pikovsky A 1998 *Phys. Rev.* E **57** 1585
Kuznetsov S, Neumann E, Pikovsky A and Sataev I 2000 *Phys. Rev.* E **62** 1995
Kuznetsov S P 2002 *Phys. Rev.* E **65** 066209
[10] Chastell P R, Glendinning P A and Stark J 1995 *Phys. Lett.* A **200** 17
Osinga H, Wiersig J, Glendinning P and Feudel U 2001 *Int. J. Bif. Chaos* **11** 3085
[11] Nishikawa T and Kaneko K 1996 *Phys. Rev.* E **54** 6114
[12] Yalçinkaya T and Lai Y-C 1996 *Phys. Rev. Lett.* **77** 5039
[13] Prasad A, Mehra V and Ramaswamy R 1997 *Phys. Rev. Lett.* **79** 4127
Prasad A, Mehra V and Ramaswamy R 1998 *Phys. Rev.* E **57** 1576
[14] Witt A, Feudel U and Pikovsky A 1997 *Physica* D **109** 180
[15] Venkatesan A, Lakshmanan M, Prasad A and Ramaswamy R 2000 *Phys. Rev.* E **61** 3641
Venkatesan A and Lakshmanan M 2001 *Phys. Rev.* E **63** 026219
[16] Negi S S, Prasad A and Ramaswamy R 2000 *Physica* D **145** 1
[17] Osinga H M and Feudel U 2000 *Physica* D **141** 54
[18] Hunt B R and Ott E 2001 *Phys. Rev. Lett.* **87** 254101
Kim J-W, Kim S-Y, Hunt B and Ott E 2003 *Phys. Rev.* E **67** 036211
[19] Kim S-Y, Lim W and Ott E 2003 *Phys. Rev.* E **67** 056203
[20] Ditto W L, Spano M L, Savage H T, Rauseo S N, Heagy J and Ott E 1990 *Phys. Rev. Lett.* **65** 533
Zhou T, Moss F and Bulsara A 1992 *Phys. Rev.* A **45** 5394
Ding W X, Deutsch H, Dinklage A and Wilke C 1997 *Phys. Rev.* E **55** 3769
Yang T and Bilimgut K 1997 *Phys. Lett.* A **236** 494
Bezruchko B P, Kuznetsov S P and Seleznev Y P 2000 *Phys. Rev.* E **62** 7828
[21] Bondeson A, Ott E and Antonsen T M 1985 *Phys. Rev. Lett.* **55** 2103
Ketoja J A and Satija I I 1997 *Physica* D **109** 70
[22] Zhou C-S and Chen T-L 1997 *Europhys. Lett.* **38** 261
Ramaswamy R 1997 *Phys. Rev.* E **56** 7294
[23] Bohr T, Bak P and Jensen M H 1984 *Phys. Rev.* A **30** 1970
[24] Toda M 1975 *Phys. Rep.* **18** 1
[25] Klinker T, Meyer-Ilse W and Lauterborn W 1984 *Phys. Lett.* A **101** 371
Kurz T and Lauterborn W 1988 *Phys. Rev.* A **37** 1029